
Article:
Al-Isaee, S. orcid.org/0000-0003-2813-7773, Iraqi, A. orcid.org/0000-0003-3060-6663 and Lidzey, D. (2023) Synthesis and characterisation of a new series of 2,6-linked-anthracene–benzothiadiazole based polymers for organic solar cells applications. Tetrahedron. 133416. ISSN 0040-4020

https://doi.org/10.1016/j.tet.2023.133416

Synthesis And Characterisation of a New Series of 2,6-Linked-Anthracene–Benzothiadiazole Based Polymers for Solar Cells application.

Sulaiman Al-Isaee [a], Ahmed Iraqi [b], David Lidzey [c]

[a] *Engineering Department, University of Technology and applied Sciences-Suhar, P.O Box: 135, Postal Code: 311, Sohar, Sultanate of Oman.*
[b] *Department of Chemistry, University of Sheffield, Sheffield S3 7HF, United Kingdom*
[c] *Department of Physics and Astronomy, University of Sheffield, Sheffield S3 7RH, United Kingdom*

Abstract:

A series of medium band gap alternating donor-acceptor conjugated polymers based on 2,6-linked anthracene flanked by thienyl donor units and benzothiadiazole acceptor units **(BT)** are prepared *via* direct arylation polymerization reactions. The prepared polymers show multiple absorption bands in both solutions and thin films with optical band gaps in the range of 1.75–1.85 eV. Polymers with alkylthienylethynyl substituents on the 9,10-positions of anthracene repeated units show broader absorption spectra compared to a polymer with alkynyl substituents. Photovoltaic studies of poly[9,10-bis[2-ethynyl-5-dodcylthiophene]-anthracene-2,6-diyl-alt-4,7-di(thiophene-2-yl)benzo[c][1,2,5]thiadiazole] **PATA(D)TBT** in this series, blended with phenyl-C_{70}-butyric acid methyl ester $PC_{71}BM$ shows a power conversion efficiency PCE of 0.76% and an open circuit voltage V_{oc} of 0.54 V.

Keywords:

Conjugated polymers; optical study; electrochemical properties; XRD analysis; photovoltaic property.

1. Introduction

Polymer solar cells (PSCs) with bulk heterojunction (BHJ) structures have attracted a considerable attention during the past few decades because of their advantages of low fabrication cost, light weight, easy manufacturing and flexibility [1-3]. Blending a π-conjugated polymer as an electron donor with soluble phenyl-C_{61}-butyric acid methyl ester ($PC_{61}BM$) or phenyl-C_{71}-butyric acid methyl ester ($PC_{71}BM$) electron acceptor in BHJ solar cells are one of the most successful PSCs [4,5]. New π-conjugated polymers with low band gaps were designed and developed to exhibit good matching absorption spectra with that of the solar spectrum as well as enhanced power conversion efficiency (PCE) of PSCs [6,7]. The push-pull architecture is used as the most effective strategy to obtain low band gap polymers and to control the polymer electronic and optical properties [8]. The donor units should have relatively weak electron donating ability to afford a conjugated polymer with a low-lying highest occupied molecular orbital (HOMO) level which is favorable to produce PSCs with high open circuit voltage (V_{oc}). Furthermore, good charge mobilities can be achieved by using polymers having donor-acceptor blocks with good planarity, large π-conjugation and high molecular weights [9].

One of the explored building blocks in the literature, for the synthesis of low band gap polymers are the anthracene units. The anthracene moieties were used as weak electron donor units with their enlarged planarity and rigidity which lead to good charge transporting properties [10]. Incorporation of anthracene into conjugated polymers through its 9,10-positions such as poly(*p*-phenylene-ethynlene)-*alt*-(poly(*p*-phenylenevinylene) (PPE-PPV) (**Figure 1**) has shown good results with respect to hole carrier mobilities and power conversion efficiency (up to 3.14%) [11, 12]. However, the main backbone of this type of polymer is strongly twisted out of planarity which affects the conjugation of the polymer due to the high steric hindrance [13].

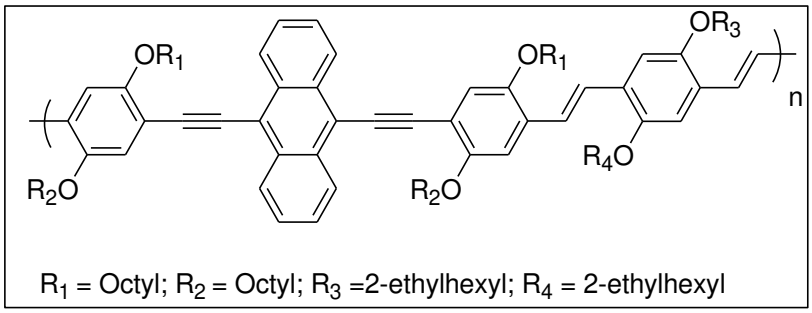

R_1 = Octyl; R_2 = Octyl; R_3 =2-ethylhexyl; R_4 = 2-ethylhexyl

Figure 1: The chemical structure of an anthracene-containing poly(*p*-phenyleneethynylene)-alt-poly(*p*-phenylene-vinylene) (PPE-PPV) copolymer.

To overcome this disadvantage, polymers based on 2,6-linked anthracene units have been used recently which improves electronic conjugation along the backbone of these polymers [14]. During the past few years, a number of polymers containing 2,6-linked anthracene units have been reported for organic photovoltaic applications [7,13, 15-18] with the highest PCE recorded by Jung *et al.* (up to 8.05%) [18]. The possibility of introducing different substitutions to the 9,10-positions on the central benzene core of the anthracene units can allow for molecular design constructing two dimensional conjugated structures.

Indeed, the need for reducing the band gap of the 2,6-linked anthracene-based polymers has led to prepare a variety of copolymers incorporating various acceptor moieties. Among these acceptor units are benzothiadiazole (BT) derivatives, which have strong electron-deficient features, due to the existence of two electron withdrawing imines (C=N) along with the bridged nitrogen atom [19]. By incorporating electron-deficient benzothiadiazole units into the polymer backbone, 2,6-linked anthracene-based polymers exhibit reduced Lowest Unoccupied Molecular Orbital (LUMO) levels and hence narrower bandgaps. Iraqi and co-workers developed polymers using 2,6-linked anthracene units with aryloxy groups at their 9,10-positions and benzothiadiazole alternate repeat unit Poly(9,10-bis(4-(dodecyloxy)phenyl)-anthracene-2,6-diyl-alt-(4,7-dithiophen-2-yl)-2',1',3'-benzothiadiazole-5,5-diyl] **PPATBT** (**Figure 2**a) [15]. The polymer exhibited a broad absorption in the range of 400–700 nm and an optical band gap of 1.84 eV. By introducing a 2-(2-hexyldecyl)-thienyl group in the 9,10-postions of the anthracene-based polymer backbone, Jung *et al*, synthesised a polymer Poly[9,10-bis[2-(2-hexyldecyl)thiophene]-anthracene-2,6-diyl-alt-(4,7-di(thiophene-2-yl)benzo[c][1,2,5]thiadiazole **PTADTBT** (**Figure 2**b) with optical band gap of 1.78 eV and PCEs reached 6.92% [18].

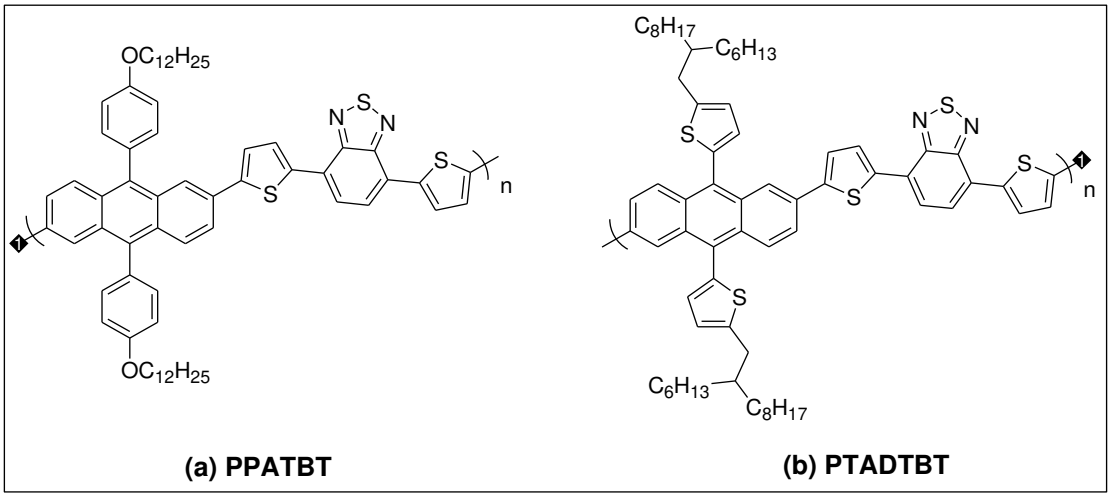

Figure 2: The Chemical structures of: (a) **PPATBT** and (b) **PTADTBT**.

In an effort to change the molecular structure to fine-tune the (V_{oc}) and short-circuit current (J_{sc}) for BHJ solar cells, three novel conjugated polymers were designed and synthesised in this work, Poly[9,10-bis[2-ethynyl-5-dodcylthiophene]-anthracene-2,6-diyl-alt-4,7-di (thiophene-2-yl)benzo[c][1,2,5]thiadiazole] **[PATA(D)TBT]**, Poly[9,10-bis[2-(ethynyl-5-butyl-octyl)thiophene]-anthracene-2,6-diyl-alt-4,7-di(thiophene-2-yl) benzo [c][1,2,5]thiadiazole] **[PATA(BO)TBT]** and Poly[9,10-di-(3-pentylundec-1-yne)-anthracene-2,6-diyl-alt-4,7-di(thiophene-2-yl)benzo[c][1,2,5]thiadiazole] **[PAA(PU)TBT]**. The polymers are substituted with 5-dodecyl-(thien-2-yl)-ethynyl, 5-(2-butyloctyl)-(thien-2-yl)-ethynyl and 3-pentylundec-1-yne side chains incorporated at the 9,10-postions of the anthracene moieties as shown in **Figure 3**. It was hoped that attaching alkylthienyl units through an acetylene spacer will extend electronic conjugation laterally as well as along the polymer chain to create a two dimensional conjugated system 2-D, which is hoped to promote planarity and light absorption resulting in a lower band gap. Furthermore, the incorporation of these substituents to the anthracene could result in enhanced charge mobility as well as good solubility of the prepared polymers in common organic solvents given the size of the alkyl substituents used.

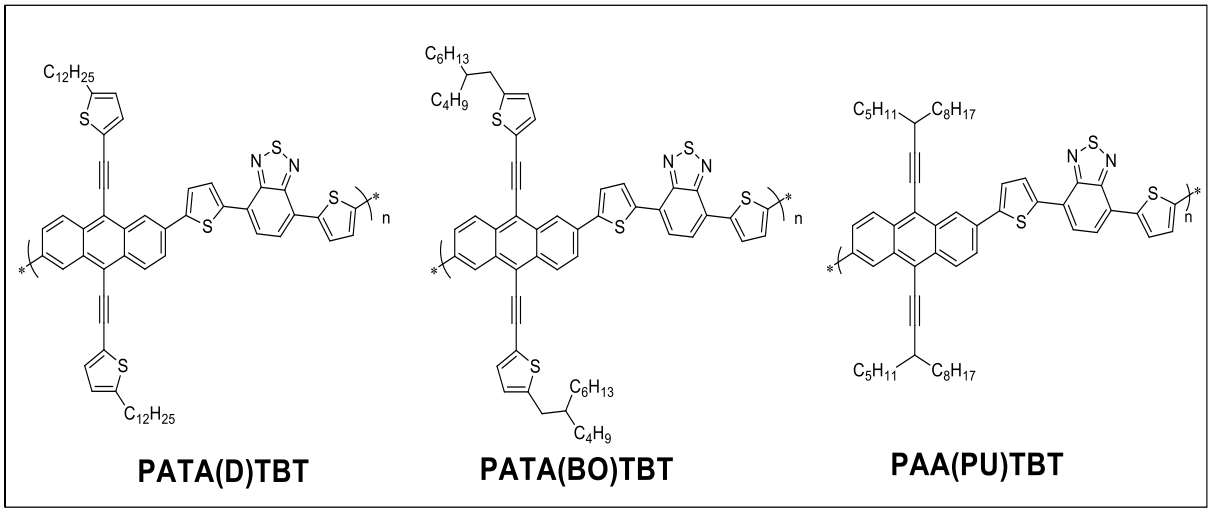

Figure 3: The Chemical structures of the target polymers, **PATA(D)TBT**, **PATA(BO)TBT**, and **PAA(PU)TBT**.

2. Experimental

2.1 Materials

Unless otherwise stated, all chemicals, reagents and solvents were obtained from commercial sources in the highest purities possible and used as received. All reactions proceeded under an argon atmosphere as standard unless stated otherwise. Anhydrous solvents used for the reactions obtained from Grubbs solvent purification system within the Chemistry Department of the University of Sheffield. 4,7-Dithien-2-yl-2,1,3-benzothiadiazole (**M4**) was synthesised according to the procedure described by Fu *et al* [20].

2.2 Measurements:

Elemental analyses were analysed by using the Perkin Elmer 2400 CHN Elemental Analyser for CHN analysis, and the Schoniger oxygen flask combustion method for sulphur and halides. In both methods, the weights submitted for the analysis were 10 mg. Fourier transform infrared spectroscopy (FTIR) and attenuated total reflectance (ATR) were recorded on a Perkin Elmer Spectrum 65 spectroscopy.

^{13}C and ^{1}H-NMR spectra of the monomers were recorded on Bruker AV 250 (250 MHz), and Bruker AV 400 (400 MHz) NMR spectrometers at room temperature in chloroform-d ($CDCl_3$) solution. NMR spectra of the polymers were recorded using Bruker Avance III HD 500 (500 MHz) at 100 °C in *1,1,2,2-tetrachloroethane-d2* solution. As an internal standard, tetramethylsilane (TMS) was used for calibrating chemical shifts (δ). The chemical shifts were measured in part per million (ppm), while the coupling constant (*J*) were given in Hertz (Hz).

GC-MS spectra were recorded on Perkin Elmer Turbomass Mass Spectrometer equipped with a Perkin Elmer Autosystem XL Gas Chromatograph. Mass spectra were obtained by the electron impact method (EI) and MALDI-TOF mass spectrometry.

Gel permeation chromatography (GPC) analysis were recorded on the equipment consisted of a Viscotek GPC_{max} VE 2001 GPC solvent/sample module, a Waters 410 Differential Refractometer and a PLgel 5 μm Mixed Column (650 mm set length) using chloroform as the eluent at rate of 1 mL/min. Polymer samples were made up as a solutions in chloroform (2 mg/mL) spiked with toluene as a reference. The RI-detection method was used to obtain the GPC curves, which was calibrated with a series of polystyrene narrow standards.

Perkin Elmer TGA-7 Thermogravimetric Analyser was used to determine TGA curves at a scan rate of 10 °C/minute under nitrogen atmosphere.

Powder X-ray diffraction were conducted on a Bruker D8 advance diffractometer with a CuKα radiation source (1.5418 A, rated as 1.6 kW). The scanning angle was recorded over the range 2–30°.

Hitachi U-2010 Double Beam UV-Visible Spectrophotometer was used to evaluate the optical properties of the polymers. The absorbance of the polymers was measured in a solution of chloroform at room temperature using quartz cuvette (l = 10 mm). Thin films of the polymers were prepared by dip coating quartz plates into around 1 mg/mL solutions in chloroform, then dried in the air and the UV-Vis absorption spectra measurements were run at room temperature.

Cyclic voltammograms (CV) were conducted using Princeton Applied Research Model 263A Potentiostat/Galvanostat. The analyses were recorded under Argon protection at approximately room temperature. A three electrode system was used for the measurements consisting of an Ag/Ag^+ reference electrode (Ag wire in 0.01 *M* $AgNO_3$ solution in the electrolyte solution), a Pt working electrode, and Pt counter electrode (Pt wire). Measurements were done in tetrabutylammonium perchlorate acetonitrile solution (0.1 *M*) on polymer thin films which made by drop casting polymer solution onto the working electrode which were left to dry in air. According to the IUPAC's recommendation, ferrocene was used as a reference redox system [21]. The energy level of Fc/Fc^+ was assumed at –4.8 eV to vacuum. The half-wave potential of Fc/Fc+ redox couple was found to be 0.08 V *vs*. Ag/Ag^+ reference electrode. The HOMO and LUMO energy level were calculated using the following equations:

$$E_{LUMO} = -[(E_{red,onset} - E_{1/2(ferrocene)}) + 4.8] \text{ eV}$$

$$E_{HOMO} = -[(E_{ox,onset} - E_{1/2(ferrocene)}) + 4.8] \text{ eV}$$

where $E_{red,onset}$ and $E_{ox,onset}$ are the onset of reduction and oxidation, respectively, relative to Ag/Ag^+ reference electrode [22].

2.3 Preparation of monomers and polymers:

2.3.1 *Synthesis of 2,6-dibromo-9,10-bis[2-ethynyl-5-dodcylthiophen-2-yl] anthracene (M1):*

In a dried round bottom flask, 2-ethynyl-5-dodcylthiophene (1.8 g, 6.5×10^{-3} mol) was dissolved in 120 mL of dry THF. *n*-BuLi (4.06 mL, 6.5×10^{-3} mol, 1.6 *M* solution in hexane) was added dropwise over 5 minutes at –78 °C. The reaction mixture was stirred for 30 minutes at room

temperature, followed by the addition of 2,6-dibromo-9,10-antharaquinone (1.07 g, 3.3×10^{-3} mol) to the mixture at –78 °C. The mixture was stirred at room temperature overnight. The reaction mixture was quenched by adding a solution of $SnCl_2$ (3.70 g, 2.0×10^{-2} mol) in 10% HCl (15 mL) and the mixture was stirred for 30 minutes at 60 °C. After completing the reaction, the solution was precipitated into methanol (MeOH) and the product was collected as an orange solid (2.45 g, 85%).

^{1}H-NMR (250 MHz, *CDCl$_3$*) δ_H/ppm: 8.69 (s, 2H), 8.41 (d, *J* = 9.0 Hz, 2H), 7.67 (d, *J* = 8.5 Hz, 2H), 7.37 (d, *J* = 3.5 Hz, 2H), 6.80 (d, *J* = 3.5 Hz, 2H), 2.90 (t, *J* = 7.5 Hz, 4H), 1.82-1.70 (m, 4H), 1.45-1.23 (m, 36H) 0.89 (t, *J* = 6.5 Hz, 6H).

Elemental Analysis (%) Calculated for $C_{50}H_{60}Br_2S_2$: C, 67.86; H, 6.84; Br, 18.05; S, 7.23. Found: C, 67.21; H, 6.63; Br, 19.09; S, 7.37. Mass (MALDI-TOF); (*m/z*) 884 (M^+).

FT-IR (cm^{-1}): 2957-2846 (aliphatic C–H stretching), 2180 (carbon, carbon triple bond stretching C≡C), 1544 and 1464 (aromatic C=C stretching), 792 (C–Br stretching), 725 (CH_2 bending).

2.3.2 *Synthesis of 2,6-dibromo-9,10-bis-[2-ethynyl-5-(2-butyl-octyl)thiophen-2-yl]-anthracene (M2):*

This product was synthesised by the same method described above for 2,6-dibromo-9,10-bis[2-ethynyl-5-dodcylthiophen-2-yl]anthracene **(M1)**. Materials used to prepare the product were; 2-ethynyl-5-(2-bytyl-octyl) thiophene (2.5 g, 9.0×10^{-3} mol), n-BuLi (2.5 M in hexane, 3.5 mL, 8.7×10^{-3} mol), 2,6-dibromo-9,10-antharaquinone (1.65 g, 4.5×10^{-3} mol) and a solution of $SnCl_2$ (3.43 g, 1.8×10^{-2} mol) in 10% HCl (15 mL). The product was collected as dark red solid (2.3 g, 58%).

^{1}H-NMR (250 MHz, *CDCl$_3$*) δ_H/ppm: 8.53 (s, 2H), 8.25 (d, *J* = 9.0 Hz, 2H), 7.58 (dd, *J* = 2.5, 9.0 Hz, 2H), 7.34 (d, *J* = 3.5 Hz, 2H), 6.79 (d, *J* = 3.5, 2H), 2.84 (d, *J* = 7.0, 4H), 1.80-1.68 (bm, 2H), 1.44-1.26 (bm, 32H) 0.99-0.90 (bm, 12 H).

^{13}C-NMR (250 MHz, *CDCl$_3$*): δ 148.43, 132.80, 132.14, 130.53, 130.10, 129.04, 128.80, 125.71, 121.82, 120.30, 117.48, 97.04, 88.86, 40.13, 34.82, 33.28, 32.96, 31.93, 29.68, 28.89, 26.64, 23.06, 22.72, 14.18, 14.16.

Elemental Analysis (%) Calculated for $C_{50}H_{60}Br_2S_2$: C, 67.86; H, 6.84; Br, 18.05; S, 7.23. Found: C, 67.06; H, 6.88; Br, 19.42; S, 6.93. Mass (MALDI-TOF); (*m/z*) 884 (M^+).

FT-IR (cm^{-1}): 2958-2847 (aliphatic C–H stretching), 2180 (C≡C stretching), 1541 and 1461 (aromatic C=C stretching), 785 (C–Br stretching), 720 (CH_2 bending).

2.3.3 *Synthesis of 2,6-dibromo-9,10-di-(3-pentylundec-1-yne)-anthracene (M3):*

This product was synthesised by the same method described for 2,6-dibromo-9,10-bis[2-ethynyl-5-dodcylthiophen-2-yl]anthracene (**M1)**. Materials used to prepare the product were; 3-pentylundec-1-yne (7.5 g, 3.4×10^{-2} mol), n-BuLi (2.5 M in hexane, 10 mL, 2.5×10^{-2} mol), 2,6-dibromo-9,10-antharaquinone (2.75 g, 7.5×10^{-3} mol) and a solution of $SnCl_2$ (4.04 g, 1.1×10^{-2} mol) in 10% HCl (15 mL). The product was purified *via* silica gel column chromatography using petroleum ether as an eluent (2.10 g, 36%).

^{1}H-NMR (400 MHz, *CDCl$_3$*) δ_H/ppm: 8.72 (d, *J*= 2.0, 2H), 8.41 (d, *J* = 9.0 Hz, 2H), 7.62 (dd, *J* = 2.0, 9.0 Hz, 2H), 2.89 (m, 2H), 1.82-1.60 (bm, 14H), 1.52-1.25 (bm, 30H) 0.97 (t, *J* = 7.0 Hz, 6H) 0.89 (t, *J* = 7.0, 6H).

^{13}C-NMR (400 MHz, *CDCl$_3$*): δ 132.95, 130.77, 130.26, 129.40, 129.14, 121.41, 118.20, 108.16, 77.68, 35.39, 35.34, 33.40, 31.95, 31.84, 29.69, 29.38, 27.92, 27.58, 22.75, 22.72, 14.16.

Elemental Analysis (%) Calculated for $C_{46}H_{64}Br_2$: C, 71.12; H, 8.29; Br, 20.57. Found: C, 70.45; H, 8.18; Br, 21.89. Mass (MALDI-TOF); (*m/z*) 776 (M^+).

FT-IR (cm^{-1}): 2957-2846 (aliphatic C–H stretching), 2180 (C≡C stretching), 1605 and 1464 (aromatic C=C stretching), 800 (C–Br stretching), 725 (CH_2 bending).

2.3.4 *Synthesis of the Poly[9,10-bis[2-ethynyl-5-dodcylthiophene]-anthracene-2,6-diyl-alt-4,7-di(thiophene-2-yl)benzo[c][1,2,5]thiadiazole] (PATA(D)TBT):*

An oven-dry sealed tube was charged with dibromo-9,10-bis[2-ethynyl-5-dodcylthiophene]anthracene (0.124 g, 0.14 × 10^{-3} mol), 4,7-di-2-thienyl-2,1,3-benzothiadiazole (0.079 g, 0.14 × 10^{-3} mol), (*o*-OMePh)$_3$P (0.0025 g, 0.0112 × 10^{-3} mol) and Pd(OAc)$_2$ (0.0026 g, 0.0028 × 10^{-3} mol), pivalic acid (0.014 g, 0.14 × 10^{-3} mol) and Cs_2CO_3 (0.14 g, 0.420× 10^{-3} mol). The tube was subjected to several cycles of vacuum followed by refilling with argon. Then, dry toluene (1.0 mL) was added and the mixture was degassed again. The polymerization was carried out at 100 °C for 2 hours under argon protection. The reaction was cooled to room temperature, diluted with 300 mL of chloroform followed by addition of ammonium hydroxide (NH_4OH) to remove residual catalyst before precipitating the reaction contents into methanol. The raw product was collected by filtration and purified using Soxhlet extraction with solvents in the order; methanol (250 mL), acetone (250 mL), hexane (250 mL), toluene (250 mL), chloroform (250 mL). The toluene fraction was concentrated (≈ 50 mL) and then poured into methanol (500 mL). The resulting mixture was stirred overnight and the solid was collected by filtration through a membrane filter to yield a dark purple powder (32 mg, 22%).

GPC (TCB): M_w = 4000, M_n = 3600, PDI = 1.1. ^{1}H-NMR ($C_2D_2Cl_4$): (δ_H/ppm): signals were not clear due to low solubility. Elemental Analysis (%) calculated for $C_{64}H_{68}N_2S_5$: C, 74.95; H, 6.68; N, 2.72; S, 15.63. Found: C, 82.36; H, 13.44. FT-IR (cm^{-1}): 3070-3045 (aromatic C–H stretching), 2951-2849 (aliphatic C–H stretching), 2114 (C≡C stretching), 1531 and 1484 (aromatic C=C stretching). 1462 (C–H bending aliphatic).

2.3.5 *Synthesis of the Poly[9,10-bis[2-(ethynyl-5-butyl-octyl)thiophene]-anthracene-2,6-diyl-alt-4,7-di(thiophene-2-yl) benzo [c][1,2,5]thiadiazole] (PATA(BO)TBT):*

The procedure for preparation of (**PATA(D)TBT**) was followed to prepare (**PATA(BO)TBT**) from **M2** (0.124 g, 0.14 × 10^{-3} mol) and **M4** (0.079 g, 0.14 × 10^{-3} mol)**.** The polymer was collected from toluene fraction as dark purple solid (33 mg, 23%).

GPC (TCB): M_w = 3200, M_n = 2100, PDI = 1.56. ^{1}HNMR ($C_2D_2Cl_4$): (δ_H/ppm); 8.79 (d, *J* = 1.5 Hz, 2H); 8.53 (d, *J* = 9.0 Hz, 2H); 8.13 (d, *J* = 4.0 Hz, 2H); 7.90 (bm, *J* = 9.0, 2.0 Hz, 2H); 7.59 (d, *J* = 4.0 Hz, 2H); 7.43 (t, *J* = 4.0 Hz, 2H); 7.17 (dd, *J* = 5.0, 1.5 Hz, 2H); 6.84 (d, *J* = 3.5 Hz, 2H); 2.87 (d, *J* = 6.5 Hz, 4H); 1.79-1.73 (m, 2H); 1.45-1.28 (bm, 32H); 0.95-0.86 (bm, 12H). Elemental Analysis (%) calculated for $C_{64}H_{66}N_2S_5$: C, 75.10; H, 6.50; N, 2.73; S, 15.66. Found: C, 69.67; H, 5.71; N, 3.78; S, 17.90. FT-IR (cm^{-1}): 3073-3051 (aromatic C–H stretching), 2951-2852 (aliphatic C–H stretching), 2182 (C≡C stretching), 1615-1484 (aromatic C=C stretching). 1462 (C–H bending aliphatic).

2.3.6 *Poly[9,10-di-(3-pentylundec-1-yne)-anthracene-2,6diyl-alt-4,7-di (thiophene-2-yl)benzo[c][1,2,5]thiadiazole](PAA(PU)TBT):*

The procedure for the synthesis of (**PATA(D)TBT**) was followed to synthesis (**PAA(PU)TBT**) from **M3** (0.11 g, 0.14 × 10^{-3} mol) and **M4** (0.079 g, 0.14 × 10^{-3} mol)**.** The polymer was collected from chloroform fraction as dark purple solid (55 mg, 43%).

GPC (TCB): M_w = 3300, M_n = 2200, PDI = 1.52. ^{1}HNMR ($C_2D_2Cl_4$): (δ_H/ppm); 8.89 (d, *J* = 1.5 Hz, 2H); 8.59 (d, *J* = 9.0 Hz, 2H); 8.19 (d, *J* = 4.0 Hz, 2H); 7.89 (bm, 2H); 7.61 (d, *J* = 4.0 Hz, 2H); 7.22 (dd, *J* = 5.0, 3.5 Hz, 2H); 3.03-2.88 (bm, 2H); 1. 93-1.18 (bm, 46H); 0.99-0.78 (bm, 12H). Elemental Analysis (%) calculated for $C_{60}H_{70}N_2S_3$: C, 78.73; H, 7.71; N, 3.06; S, 10.50. Found: C, 73.83; H, 6.93; N, 3.57; S, 12.28. FT-IR (cm^{-1}): 3048 (aromatic C–H stretching), 2954-2849 (aliphatic C–H stretching), 2107 (C≡C stretching), 1615-1488 (aromatic C=C stretching). 1465 (C–H bending aliphatic).

3. Results and Discussion

3.1 Polymer Synthesis:

To obtain our desired alternating copolymers, we employed direct arylation coupling polymerisation using 2,6-dibromo-anthracene derivatives and 4,7-bis(thiophen-2-yl) benzo[c][1,2,5]-thiadiazole (**M4**). The synthetic routes of **M1**, **M2** and **M3** and their corresponding polymers are outlined in **scheme 1**. 4,7-Bis(thiophen-2-yl) benzo[c][1,2,5]-

thiadiazole (**M4**) was prepared according to a procedure by Fu *et al* [20]. The purity and chemical structure of the monomers were confirmed by ^{1}H-NMR, ^{13}C-NMR, FT-IR spectroscopy, elemental analysis and mass spectrometry.

Scheme 1 outlines the synthesis of polymers **PATA(D)TBT**, **PATA(BO)TBT**, and **PAA(PU)TBT** *via* direct arylation polymerization in yields between 22% and 43%. $Pd(OAc)_2$ and tri(*o*-tolyl)phosphine were used as the catalyst in the presence of Cs_2CO_3 base and pivalic acid and toluene as the solvent. All the polymers were purified by Soxhlet extraction and toluene fractions were collected, reduced in *vacuo,* and precipitated in methanol. The rather low yields of these polymers are ascribed to their low solubility. Incorporating the arylethynyl and alkynyl substituents on the anthracene units did not provide high solubilities to these polymers. This suggested that the incorporation of these substituents on the anthracene units *via* acetylene spacers led to enhance the planarity of the resulting polymers leading to strong π-π stacking between polymer chains which affected their solubility in common organic solvents. It is worth to note that, even the quantities of these polymers which were extracted in toluene fractions, exhibited very low solubility at room temperature in common organic solvents such as chlorobenzene and chloroform. This is why it was only possible to fabricate photovoltaic devices from **PATA(D)TBT**.

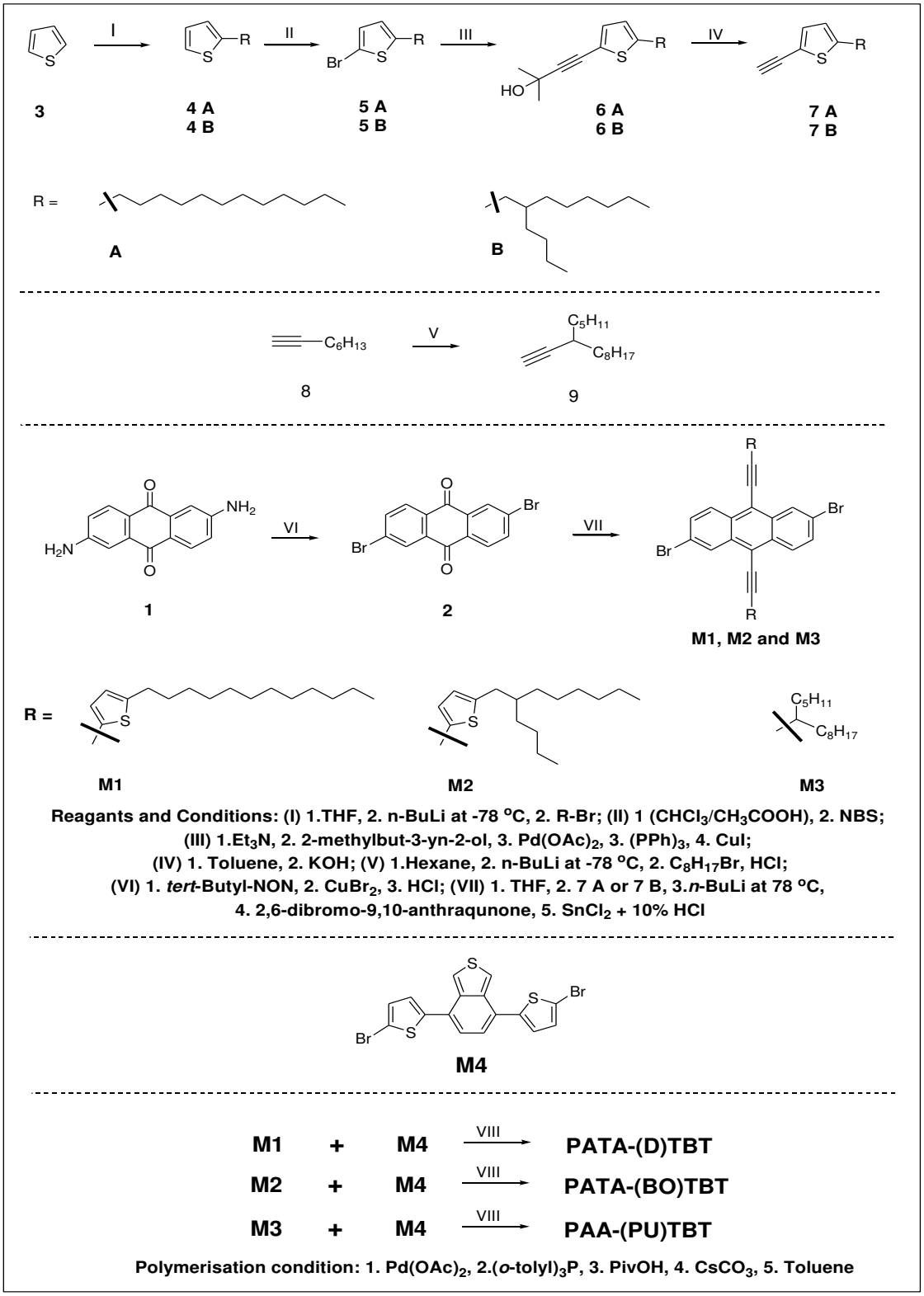

Scheme 1: The reaction pathway to the anthracene monomers and their corresponding polymers.

All polymers were characterised by ^{1}H-NMR, IR, and elemental analysis to confirm their chemical structures. The number average molecular weights (M_n) of the polymers were determined using gel permeation chromatography (GPC) relative to polystyrene standards using 1,2,4-trichlorobenzene as the eluent (**Table 1**). Polymer **PPATBT**, prepared by Iraqi *et al*. [15], (an analogous polymer to our polymers which has 4-dodecyloxy-phenyl substituents on the anthracene units) had an M_n of 3500 Da which is very close to the molecular weights of the new polymers prepared in this study. Surprisingly, polymer **PTADTBT** prepared by Jung *et al.* [18] showed a higher M_n value of 41100 Da compared to those obtained for polymers presented in this work. This difference in the M_n can be attributed to the twisting out of planarity of the bulky branched 2-hexyldecyl-thienyl substituents attached to the anthracene units at its 9,10 positions and the anthracene units in **PTADTBT**. As a result, the π-π stacking between the polymers chains was disrupted leading to more soluble polymer with higher M_n values.

Table 1: GPC data and TGA data of the polymers.

Polymer	Yield (%)	M_n (Da)[a]	M_w (Da)[a]	PDI[b]
PATA(D)TBT	22	3600	4000	1.2
PATA(BO)TBT	23	2100	3200	1.56
PAA(PU)TBT	43	2200	3300	1.52

[a] Measurements conducted on the polymers using a differential refractive index (DRI) detection method.

[b] Polydispersity index.

3.2 Thermal Analysis:

Thermal stability of the polymers was investigated *via* thermal gravimetric analysis (TGA) under N_2 atmosphere. The three polymers displayed high thermal stability with 5% loss in excess of 300 °C as shown in **Figure 4**. Polymers, **PTAT(D)TBT** and **PTAT(BO)TBT** show degradation temperatures of 332 and 401 °C, respectively. Whereas, **PAA(PU)TBT** with alkynyl substituents attached to the anthracene moiety has a degradation temperature of 352 °C. This indicates that all the polymers are thermally stable enough to be fabricated into organic photovoltaic devices.

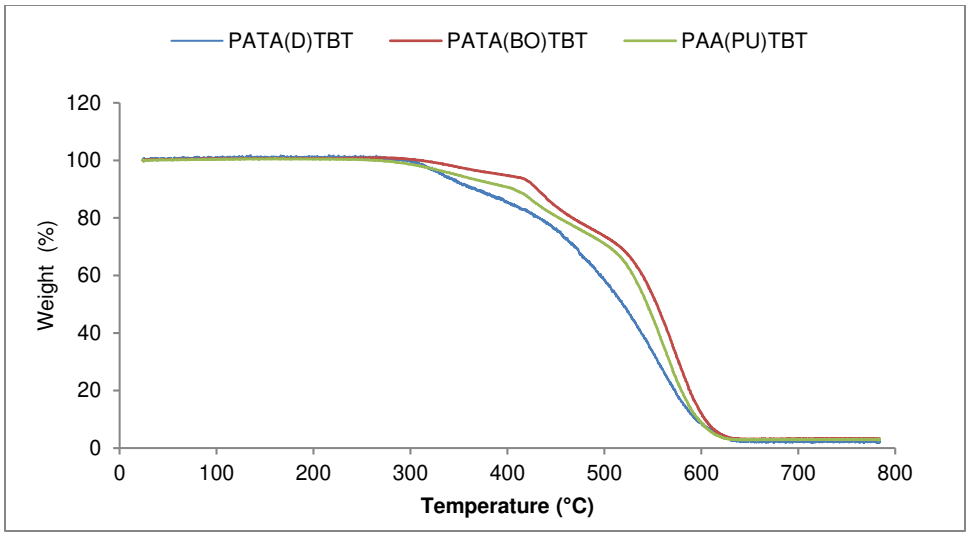

Figure 4: TGA plots of **PATA(D)TBT**, **PATA(BO)TBT** and **PAA(PU)TBT**.

3.3 Optical Properties:

The UV-Vis spectra of the three polymers in chloroform solutions and as thin films are displayed in **Figure 6**, and all their optical data are summarised in **Table 2**. The three polymers show multiple absorption bands in the range 300-650 nm either in the solution phase or as thin films. The absorption bands in the higher energy region are attributed to the π-π* transitions [23], while the low-energy absorptions are originated from intramolecular charge transfer between the anthracene dithienyl donor units and BT acceptor units [24]. These absorption bands are bathochromically shifted in the case of thin films due to the enhancement in the interchain packing in the solid state. **PATA(BO)TBT** and **PAA(PU)TBT** have shown clear shoulder peaks already in dilute solutions at long-wavelengths around 642 and 517 nm respectively, indicating the existence of aggregation in the solution phase due to stacking of polymer chains [15]. This provides a good evidence for the backbone planarisation enhancement upon the use of acetylenic substituents into the polymer backbones. Also, the existence of these shoulders in the solution phase can explain the low solubility of these polymers as well as their low molecular weights. These shoulder absorption peaks become more pronounced in the spectra of the thin films of the three polymers.

Table 2: UV-Vis data and optical band gaps of the polymers **PATA(D)TBT**, **PATA(BO)TBT** and **PAA(PU)TBT**.

Polymer	λ_{max} solution (nm)	ε^a (M^{-1} cm^{-1})	λ_{max} film (nm)	E_g^{opt} film (eV)[b]
PATA(D)TBT	330, 382, 475	3.90×10^{-4}	384, 493, 638	1.75
PATA(BO)TBT	333, 377, 470	3.90×10^{-4}	393, 493, 634	1.80
PAA(PU)TBT	359, 448, 516	3.48×10^{-4}	370, 560	1.85

[a] Molar absorptivity measured at λ_{max} in chloroform. [b](E_g^{opt}) optical bandgap, calculated from the onset of the absorption bands on solid films.

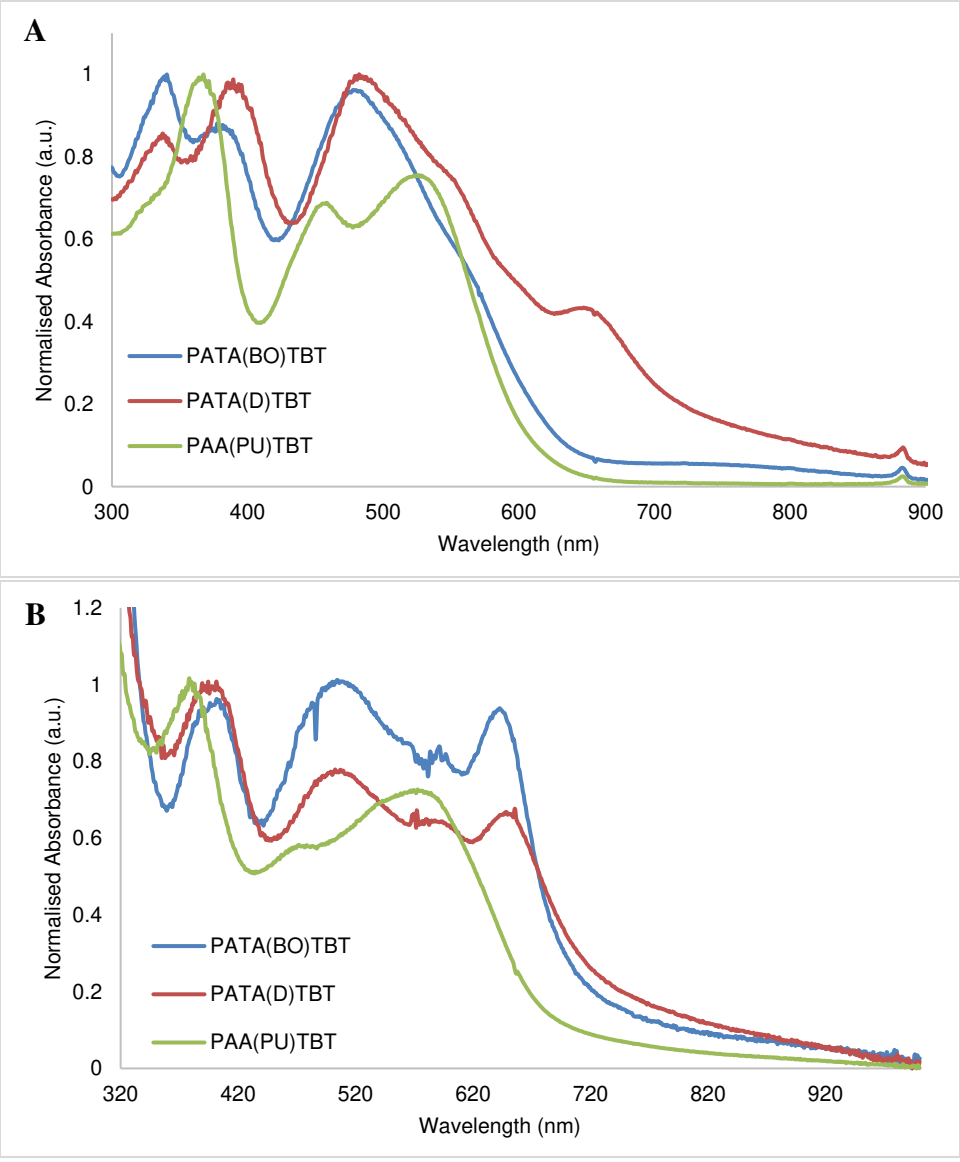

Figure 5: Normalised UV-Vis absorption spectra of **PATA(D)TBT**, **PATA(BO)TBT** and **PAA(PU)TBT** in : (A) chloroform solutions; and (B) thin films.

The nature of the three ethynyl substituents 2-ethynyl-5-dodcylthiophene (**7A**), 2-ethynyl-5-(2-bytyl-octyl) thiophene (**7B**) and 3-pentylundec-1-yne (**9**) **(Scheme 1)** attached to the backbone of the polymers seem to have an influence in their optical properties. In films, the peak of absorption (λ_{max}) of the polymer **PAA(PU)TBT** is about 560 nm, whereas, the λ_{max} of the polymers **PATA(D)TBT** and **PATA(BO)TBT** show red shifts by 78 and 74 nm, respectively. The red-shifted absorptions of **PATA(D)TBT** and **PATA(BO)TBT** can be ascribed to the additional thienyl units attached to the acetylene substituents as side chains on the anthracene units, which extend the electronic conjugation laterally on these polymers. Using the linear alkylthienylethynyl (**7A**) substituents in **PATA(D)TBT** resulted in the enhancement of the stacking of polymer backbones leading to a reduced optical band gap relative to those of **PATA(BO)TBT** and **PAA(PU)TBT**. The optical band gaps (E_g^{opt}) of the polymers with different substituents were (**7A**) (1.75 eV) < (**7B**) (1.80 eV) < (**9**) (1.85 eV).

It is worth to mention, the molar absorption coefficients of the polymers **PATA(D)TBT** and **PATA(BO)TBT** ($\varepsilon = 3.90 \times 10^{-4}$ M^{-1} cm^{-1} for both) are higher than that of **PAA(PU)TBT** (3.48×10^{-4} M^{-1} cm^{-1}) indicating that the amount of photons absorbed by the former polymers are higher. All these results suggest that introducing arylethynyl groups to the polymer backbone helps in delocalising π-electrons to the conjugated side substituents which enlarged the π-conjugation more effectively. As a result, **PATA(D)TBT** and **PATA(BO)TBT** with conjugated side groups will have larger conjugated area compared to **PAA(PU)TBT** which resulted in a more effective interchain π-π overlapping leading to better optical properties [25].

3.4 Electrochemical Characterisation:

The optical properties of conjugated polymers can provide the energy separation of their frontier orbitals i.e their energy band gaps [26]. However, to achieve more details on the positions of their HOMO and LOMO levels, the reduction and oxidation potentials of the conjugated polymers were measured using cyclic voltammetry (CV). It is a very important tool which provides us with very important information for a better understanding of their photovoltaic performances [26].

The HOMO and LUMO energy levels of the polymers were determined by CV measurements which were achieved under argon by using a solution of tetrabutylammonium perchlorate in acetonitrile as the supporting electrolyte with a Pt disc as a working electrode, Ag/Ag^+ as reference electrode and counter electrode, Ferrocene (Fc) was used as the reference redox standard. According to the literature, the redox potential of Fc/Fc^+ is –4.8 eV below the vacuum level [27]. The half-way potential of Fc/Fc^+ was measured to be 0.083 eV with respect to Ag/Ag^+ reference electrode. Therefore, the HOMO and LUMO energy levels were calculated using the following equations:

$$E_{LUMO} = -[(E_{red,onset} - E_{1/2(Fc)}) + 4.8] \text{ eV}$$

$$E_{HOMO} = -[(E_{ox,onset} - E_{1/2(Fc)}) + 4.8] \text{ eV}$$

where $E_{red,onset}$ and $E_{ox,onset}$ are the onsets of reduction and oxidation of the polymers, respectively, relative to Ag/Ag^+ reference electrode. The cyclic voltammograms of the three polymers are displayed in **Figure 6** and the detailed electrochemical data is summarised in **Table 3**.

The E_{HOMO}/E_{LUMO} levels of the polymers **PATA(D)TBT**, **PATA(BO)TBT** and **PAA(PU)TBT** were found to be –5.39/–3.52, –5.41/–3.55 and –5.42/–3.50 eV, respectively. This obvious similarity in the electrochemical properties of the polymers indicates that there was no significant impact of the attached substituents into the backbone of these polymers. The values of the HOMO levels of these polymers are comparable to similar polymers with anthracene repeat units having alkylaryl substituents on their 9,10-positions and benzothiadiazole units (**PPATBT**, HOMO at –5.44 eV and **PTADTBT**, HOMO at –5.40 eV) [15, 18].

Table 3: The energy levels and electrochemical band gaps of the polymers.

Polymers	HOMO (eV) [a]	LUMO (eV) [b]	E_g^{elece} (eV) [c]
PATA(D)TBT	–5.39	–3.52	1.87
PATA(BO)TBT	–5.41	–3.55	1.86
PAA(PU)TBT	–5.42	–3.50	1.92

[a] HOMO position (*vs. vacuum*) determined from onset of oxidation. [b] LUMO position (*vs. vacuum*) determined from onset of reduction. [c] Electrochemical energy gap of the polymers.

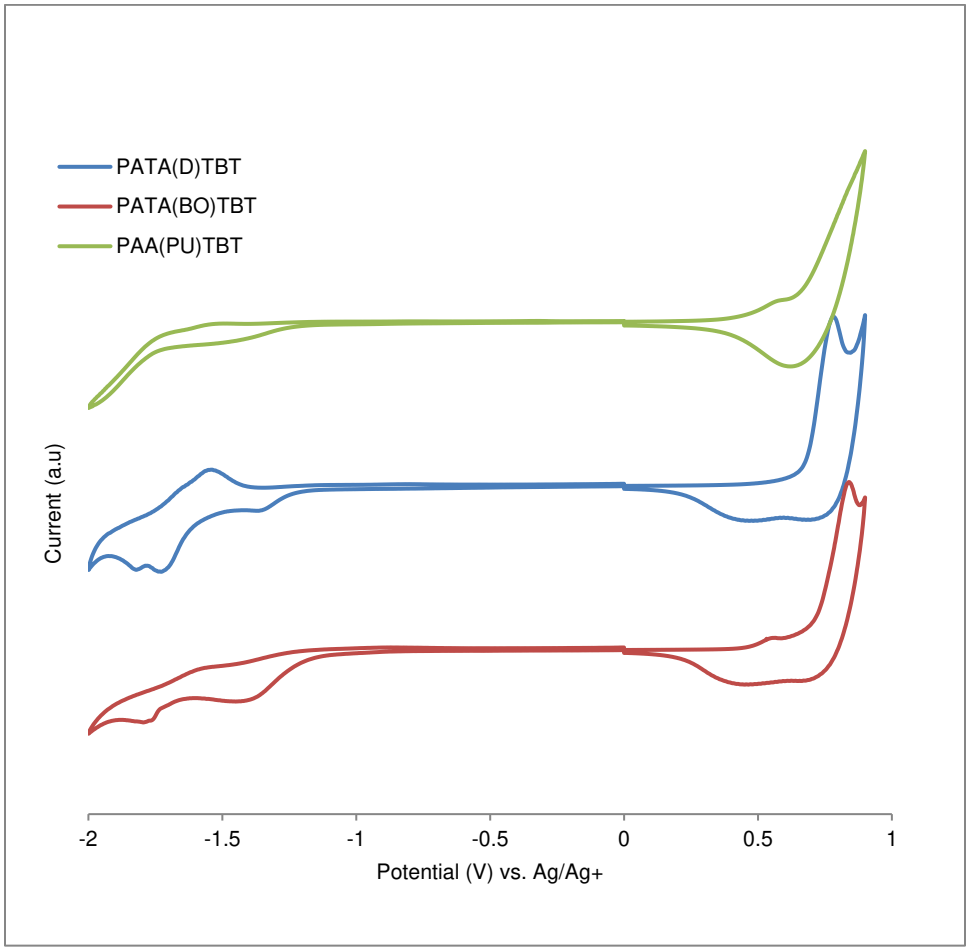

Figure 6: Cyclic voltammograms of **PATA(D)TBT**, **PATA(BO)TBT** and **PAA(PU)TBT**.

However, the LUMO levels of the three polymers are relatively higher than **PTADTBT** (LUMO at –3.62 eV) synthesised by Jung and co-workers [18]. This difference could be due to the high molecular weight of **PTADTBT**. According to a previous literature, the LUMO level of a polymer become much deeper when compared to the HOMO level as the molecular weight increases [28, 29]. Kim *et al*, ascribed that to the molecular orbital hybridisation of the donor and acceptor units which resulted in localisation of the LUMO level on the electron-rich unit as the M_n of the polymer increases [29].

On the other hand, **PPATBT** synthesised by Iraqi *et al.* [15] had a LUMO level of –3.21 eV higher than the LUMO levels of the polymers presented in this work; even though the polymers have a comparable low molecular weight. Clearly, modification of these polymers by replacing

4-dodecyloxyphenyl groups attached to the anthracene units with arylethynyl or alkynyl groups resulted in improving the electronic properties of this new class of polymers. It seems that using acetylene units to connect alkylthienyl groups and the polymer backbone leads to an extension of the conjugation of the polymer in 2-D which enhance the resonance effect. Therefore, the polymers which incorporate alkylthienylethynyl or alkynyl groups induce efficient intramolecular charge separation leading to a considerable decline in their LUMO energy levels [28].

3.5 X-ray Diffraction studies:

The crystallinity of the three polymers was investigated by X-ray powder diffraction (XRD) (**Figure 7**). Diffraction peaks for **PATA(D)TBT**, **PATA(BO)TBT** and **PAA(PU)TBT** appeared in the wide angle region at 2θ of 22.01, 20.74° and 22.33°, respectively, reflecting the π-π stacking distances between the polymer chains which are calculated using Bragg's equation to be 4.03, 4.28 and 3.98 Å, respectively. The intensity of the diffraction peak of **PATA(BO)TBT** in the wide angle region is larger than the other two polymers indicating that **PATA(BO)TBT** has better crystallinity [30]. Also it is worth to mention that, **PATA(BO)TBT** display a sharp peak at 2θ value of 4.13° which corresponds to a distance of 21.37 Å. According to previous studies on different conjugated polymers, this value could be attributed to the distance between polymer backbones separated by the alkyl chains [30, 31]. It is believed that the incorporation of the substituents through acetylene groups resulted in enhanced π-π stacking and intermolecular interactions of these polymers. These results may provide a good explanation for the low solubility of these polymers in common organic solvents and hence their low molecular weights. It is anticipated that the miscibility of these polymers with electron acceptor $PC_{70}BM$ will be very low, and therefore it might be difficult to fabricate them into organic solar cells in view of their low solubility.

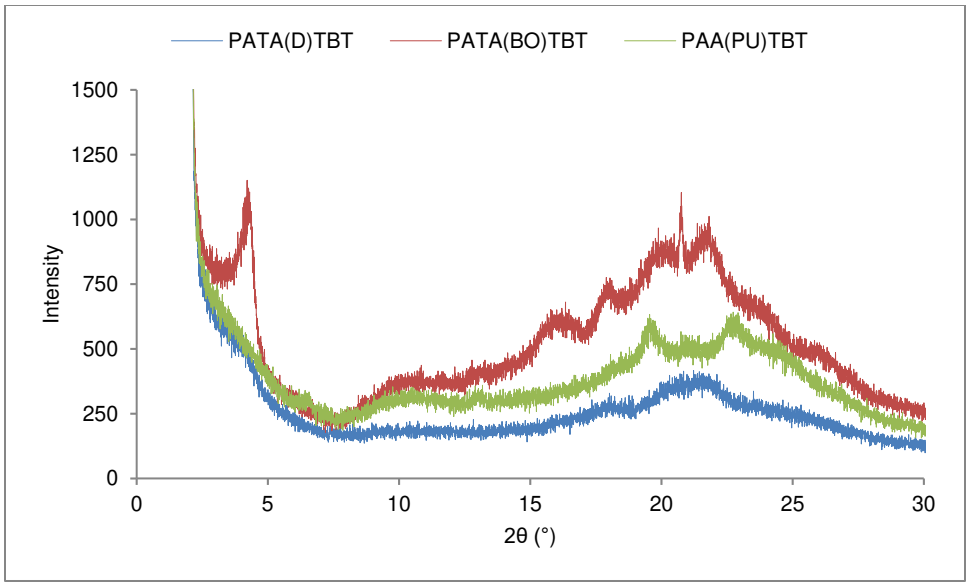

Figure 7: Powder X-ray diffraction scans of the polymers **PATA(D)TBT**, **PATA(BO)TBT** and **PAA(PU)TBT.**

3.6 Photovoltaic Device Properties:

The photovoltaic performance of the polymers were evaluated using a series of glass/ITO/PEDOT:PSS/polymer : $PC_{70}BM$ (1 : 3)/Ca/Al polymer solar cells devices. Preparation of uniform films from **PATA(BO)TBT** and **PAA(PU)TBT** were difficult to achieve as the polymers formed aggregates at the surface of the film after spin coating due to their low solubilities. **PATA(D)TBT** was the only polymer in the series that was possible to process into devices. The *J–V* curve of the **PATA(D)TBT** device is shown in **Figure 8**, and the device parameters are listed in **Table 4**. The performance of the device was quite modest in comparison to its counterparts **PTADTBT** prepared by Jung and co-worker and **PPATBT** prepared by Iraqi group [15, 18]. The polymer provided a device with an open circuit voltage (V_{oc}) of 0.54 V, a short circuit current density (J_{sc}) of 2.76 mA/cm^2, a fill factor (FF) of 51% and a power conversion efficiency of 0.76%.

Table 4: Photovoltaic performance of **PATA(D)TBT** measured under a simulated photovoltaic light with 1000 Wm^{-2} the illumination (AM 1.5).

Polymer	Polymer : $PC_{71}BM^{a}$ (w/w)	Solvent	J_{sc} (mA cm^{-2})	V_{oc} (V)	FF (%)	PCE (%)
PATA(D)TBT	1 : 3	CB[b]	−2.76	0.54	51	0.76

[a] Polymer : $PC_{71}BM$ weight ratio. [b] chlorobenzene.

It is believed that the low V_{oc} of **PATA(D)TBT** compared to **PTADTBT** (V_{oc} = 0.92 V) can be ascribed to its poor solubility which resulted in formation of a non-uniform film. To support the previous assumption by comparison between the two devices through the so-called fill factor (FF). The lower fill factor of **PATA(D)TBT** seemingly due to the poor packing of the polymer chains in the device and probably a low charge mobility [15]. In addition, according to Hoppe *et al.* not only the materials' energy levels can affect the V_{oc} values, it is also a sensitive function of the energy level alignments between organic-metal electrodes interfaces [32]. So, the other possible reason that can be attributed to this difference in V_{oc} values between **PATA(D)TBT** and **PTADTBT** is the device structures used to investigate the photovoltaic properties. In fact, the V_{oc} of **PATA(D)TBT** is very close to the V_{oc} of **PPATBT** (V_{oc} = 0.59 V) prepared in Iraqi group where they have used a similar device structure to measure the photovoltaic performance of their polymer [15].

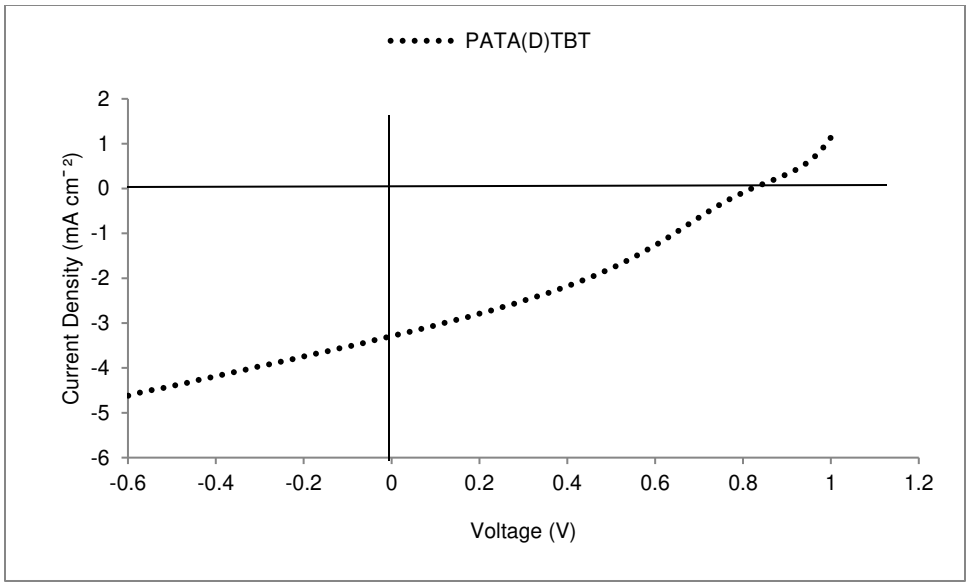

Figure 8: *J-V* characteristic curve of the organic solar cell device fabricated from **PATA(D)TBT**.

4. Conclusion:

In summary, a series of 2,6-linked anthracene derivatives based polymers were synthesised by direct arylation polymerisation with dithienyl-benzo[*c*]-[1,2,5]thiadiazole to yield **PATA(D)TBT**, **PATA(BO)TBT** and **PAA(PU)TBT**. The influence of the attached groups into the 9,10 positions of the anthracene unit was studied by UV-visible spectroscopy, cyclic voltammetry and X-ray diffraction techniques. The three polymers display a limited solubility in common organic solvent at room temperature; a consequence of the lack of solubilising groups on the **TBT** units. As a result, the fabrication of photovoltaic devices using **PATA(BO)TBT** and **PAA(PU)TBT** through solution processing were not possible. A comparison between **PAA(PU)TBT** which possesses alkynyl groups at 9,10-positions of anthracene repeat units, and the polymers with arylethynyl substituents (**PATA(D)TBT** and **PATA(BO)TBT**) indicates that the later polymers have greater electronic conjugation and lower optical band gaps. The electrochemical properties of the polymers were highly comparable; an indication of the lack of a significant influence of these attached groups on the position of the HOMO and LUMO energy levels of the polymers. Polymer solar cell based on **PATA(D)TBT** blended with $PC_{70}BM$ has shown a PCE of 0.76% and V_{oc} of 0.54 V. These low values can be attributed to the low

solubility of the polymer which presents proceesing difficulties and a poor morphology of active layers in polymer photovoltaic devices.

The processability of this class of polymers is clearly an issue that needs to be addressed. Addition of solublising groups on the benzothiadiazole repeat units could help in the preparation of polymers with enhanced processability.

5. References:

1. V. Gopalakrishnan, D. Balaji, M. S. Dangate, *ECS Journal of Solid State Science and Technology*, 2022, **11**(3), 035001.
2. T. Gokulnath, J. Choi, H. Y. Park, K. Sung, Y. Do, H. Park, S. H Jin. *Nano Energy*, 2021, ***89***, 106323.
3. C. Liu, W. Cai, X. Guan, C. Duan, Q. Xue, L. Ying, F. Huang and Y. Cao, *Polymer Chemistry*, 2013, **4**, 3949-3958.
4. A. Cardone, C. Martinelli, M. Losurdo, E. Dilonardo, G. Bruno, G. Scavia, S. Destri, P. Cosma, L. Salamandra and A. Reale, *Journal of Materials Chemistry A*, 2013, **1**, 715-727.
5. L. Bian, E. Zhu, J. Tang, W. Tang and F. Zhang, *Progress in Polymer Science*, 2012, **37**, 1292-1331.
6. C. Zhao, J. Wang, J. Jiao, L. Huang, J. Tang, *Journal of Materials Chemistry C*, 2020 ***8***(1), 28-43.
7. D. SungáChung, D. HoonáLee, N. SungáCho and C. EonáPark, *Chemical Communications*, 2010, **46**, 1863-1865.
8. P. Ding, C. C. Chu, Y. Zou, D. Xiao, C. Pan and C. S. Hsu, *Journal of Applied Polymer Science*, 2012, **123**, 99-107.
9. L. Dou, C.-C. Chen, K. Yoshimura, K. Ohya, W.-H. Chang, J. Gao, Y. Liu, E. Richard and Y. Yang, *Macromolecules*, 2013, **46**, 3384-3390.

10. C. Liu, W. Xu, X. Guan, H.-L. Yip, X. Gong, F. Huang and Y. Cao, *Macromolecules*, 2014.
11. D. A. Egbe, S. Turk, S. Rathgeber, F. Kuhnlenz, R. Jadhav, A. Wild, E. Birckner, G. Adam, A. Pivrikas and V. Cimrova, *Macromolecules*, 2010, **43**, 1261-1269.
12. J. B. Lee, K. H. Kim, C. S. Hong and D. H. Choi, *Journal of Polymer Science Part A: Polymer Chemistry*, 2012, **50**, 2809-2818.
13. W. Cui, Y. Zhao, H. Tian, Z. Xie, Y. Geng and F. Wang, *Macromolecules*, 2009, **42**, 8021-8027.
14. J. Sun, J. Chen, J. Zou, S. Ren, H. Zhong, D. Zeng, J. Du, E. Xu and Q. Fang, *Polymer*, 2008, **49**, 2282-2287.
15. A. Abdulaziz, *Chemical Communications*, 2013, **49**, 2252-2254.
16. J. Y. Ma, H. J. Yun, S. O. Kim, G. B. Lee, H. Cha, C. E. Park, S. K. Kwon and Y. H. Kim, *Journal of Polymer Science Part A: Polymer Chemistry*, 2014, **52**, 1306-1314.
17. J. W. Jung and W. H. Jo, *Polymer Chemistry*, 2015, **6**, 4013-4019.
18. J. W. Jung, F. Liu, T. P. Russell and W. H. Jo, *Advanced Energy Materials*, 2015.
19. H. Medlej, H. Awada, M. Abbas, G. Wantz, A. Bousquet, E. Grelet, K. Hariri, T. Hamieh, R. C. Hiorns and C. Dagron-Lartigau, *European Polymer Journal*, 2013, **49**, 4176-4188.
20. B. Fu, J. Baltazar, Z. Hu, A.-T. Chien, S. Kumar, C. L. Henderson, D. M. Collard and E. Reichmanis, *Chemistry of Materials*, 2012, **24**, 4123-4133.
21. G. Gritzner, *Pure and Applied Chemistry*, 1990, **62**, 1839-1858.
22. L. Cartwright, H. Yi and A. Iraqi, *New Journal of Chemistry*, 2016, **40**, 1655-1662.
23. C. Liu, W. Xu, X. Guan, H.-L. Yip, X. Gong, F. Huang and Y. Cao, *Macromolecules*, 2014, **47**, 8585-8593.
24. R. Qin, W. Li, C. Li, C. Du, C. Veit, H.-F. Schleiermacher, M. Andersson, Z. Bo, Z. Liu and O. Inganas, *Journal of the American Chemical Society*, 2009, **131**, 14612-14613.
25. L. Ye, S. Zhang, L. Huo, M. Zhang and J. Hou, *Accounts of chemical research*, 2014, **47**, 1595-1603.
26. K. Haubner, E. Jaehne, H. J. Adler, D. Koehler, C. Loppacher, L. Eng, J. Grenzer, A. Herasimovich and S. Scheinert, *physica status solidi (a)*, 2008, **205**, 430-439.

27. P. Deng, L. Liu, S. Ren, H. Li and Q. Zhang, *Chemical Communications*, 2012, **48**, 6960-6962.
28. L. Cartwright, L. J. Taylor, H. Yi, A. Iraqi, Y. Zhang, N. W. Scarratt, T. Wang and D. G. Lidzey, *RSC Advances*, 2015, **5**, 101607-101615.
29. B. G. Kim, X. Ma, C. Chen, Y. Ie, E. W. Coir, H. Hashemi, Y. Aso, P. F. Green, J. Kieffer and J. Kim, *Advanced Functional Materials*, 2013, **23**, 439-445.
30. C. Kang, J. Zhang, H. Dong, W. Hu and Z. Bo, *Journal of Materials Chemistry C*, 2015, **3**, 12083-12089.
31. L. Cartwright, A. Iraqi, Y. Zhang, T. Wang and D. G. Lidzey, *RSC Advances*, 2015, **5**, 46386-46394.
32. H. Hoppe and N. S. Sariciftci, *Journal of Materials Research*, 2004, **19**, 1924-1945.